# Exact results in a lattice model of a binary reactant mixture

Peter B. Thomas*
*Department of Physics, Brookhaven National Laboratory, Upton, New York 11973*
(Received 26 September 1994)

We study phase separation in a binary mixture of two particles, which can react with each other and form a third compound. We determine the exact phase boundaries for a restricted range of the interaction parameters.

PACS number(s): 61.20.Gy, 82.60.Lf, 05.50.+q, 61.25.Hq

## I. INTRODUCTION

Phase separation in binary mixtures is a phenomenon that occurs widely in nature, as is seen for example in microemulsions [1], alcohol water mixtures [2], binary metal alloys [3], molten salts or ionic salt solutions [4], adsorbed molecules on substrates [5], etc. It has been a subject of considerable interest, both experimentally and theoretically [6,7].

It has been known that some of the above systems can be described well in terms of Ising lattice models [8] with one order parameter. However, there are also binary systems that are more complicated. For example, binary alloys containing a magnetic component such as the Ni-Al or the Fe-Al alloys have two order parameters, namely, the mole fraction of aluminum and the magnetization. Both these systems are known to have over ten phases [9]. In general, systems having two or more order parameters can be expected to have a richer phase structure, which arises due to competition between the ordering mechanisms of the order parameters. In this paper, we study the equilibrium phases of a complex binary system that needs to be described in terms of two order parameters. Our model also has a rich variety of phases, and unlike the previous example, it is possible to obtain some exact results.

The model we study consists of two components $A$ and $B$, which can react with each other and form a third compound $C$. These kinds of systems are found to occur, for example, in various chemical reaction, ionic solutions, superconductors, etc. There have been mean field studies of such systems by Albeck and Gitterman [11], and studies on lattice models by Corrales and Wheeler [10]. One of the models in Ref. [10] is a special case of the class of systems we study here. Where relevant, our results are in qualitative agreement with theirs, which will be discussed in the appropriate contexts.

In our model, we treat the compound $C$ as an independent entity, which interacts with other neighboring particles of type $A$, $B$, and $C$. One may alternatively think of this model as a binary lattice gas that has additional effective three- and four-body interactions. This is not unreasonable, as one does occasionally encounter interactions that involve more than two particles. For example, when an ionic molecule is in the presence of a charged particle it gets polarized, which is a three-body interaction. Taking another example, in an Fe-Al alloy the ferromagnetic exchange interaction between two iron particles is altered by the presence of nearby aluminum particles, which has been written in terms of effective three- and four-body interactions in a Monte Carlo study by Schmid and Binder [12]. However, we can also justify the inclusion of many-body interactions by the discretization approximation to a lattice gas. It is in fact quite common to study models in which the many-body interactions do not necessarily have a microscopic origin, but are simply effective parameters, giving rise to the experimentally observed properties. This approach has been discussed by Zunger in Ref. [6]. It would thus be useful to have exact results in models having many-body interactions.

The paper is organized as follows. In Sec. II we describe our model and show that in a restricted region of parameter space, it can be mapped on to two interacting Ising models. This enables us to obtain exact results in some special cases, which we describe in Secs. III and IV. In Sec. V, we conclude.

## II. MODEL

We consider a lattice model of two kinds of particles, $A$ (square loops) and $B$ (small squares), which is illustrated in Fig. 1. Multiple occupancy of $A$ and $B$ type particles is forbidden. It is however possible for a particle $B$ to be in the same site as a particle, $A$, representing the formation of the compound $C$. That is, the particles $A$ and $B$ are assumed to be able to reversibly bind together according to the equation

$$A+B\rightleftharpoons C\ . \tag{1}$$

Let $-\mu_C$ be the energy associated with the forward reaction involving the formation of the compound $C$. The components $A$ and $B$ react with each other with energies $\varepsilon_{AA}$, $\varepsilon_{BB}$, and $\varepsilon_{AB}$. The compound $C$ is assumed to behave independently and in our model, one can equivalently think of the system as having effective three-body and four-body interactions. Let $\varepsilon_{AC}$ and $\varepsilon_{BC}$ be the strengths of the two effective three-body interactions, and $\varepsilon_{CC}$ be the strength of the effective four-body interaction. The partition function of the system is

*Internet: thomas@cmth.phy.bnl.gov

 

$$Z=\sum_{\{n_i\},\{\tau_i\}}\exp\left[-\beta\sum_{\langle ij\rangle}[\varepsilon_{AA}n_in_j+\varepsilon_{BB}\tau_i\tau_j+\varepsilon_{CC}\gamma_i\gamma_j+\varepsilon_{AB}(n_i\tau_j+\tau_in_j)+\varepsilon_{AC}(n_i\gamma_j+\gamma_in_j)+\varepsilon_{BC}(\tau_i\gamma_j+\gamma_i\tau_j)]\right.$$
$$\left.+\beta\sum_i(\mu_An_i+\mu_B\tau_i+\mu_C\gamma_i)\right], \tag{2}$$

where $\beta=1/T$ is the inverse temperature; $n_i$ and $\tau_i$ are indicator variables for the presence of the $A$ or $B$ components at the site $i$ and can be either 1 or 0. $\mu_A$ and $\mu_B$ are the fugacities of the $A$ and $B$ particles. The binary variable $\gamma_i$ signals the presence of absence of the compound $C$ at site $i$ and is defined by

$$\gamma_i=n_i\tau_i\ . \tag{3}$$

We note that the total interaction between $A$ and $C$ particles is $(\varepsilon_{AC}+\varepsilon_{AA}+\varepsilon_{AB})$, that between $B$ and $C$ particles it is $(\varepsilon_{BC}+\varepsilon_{AB}+\varepsilon_{BB})$, and that between two $C$ particles it is $(\varepsilon_{CC}+\varepsilon_{AA}+\varepsilon_{BB}+2\varepsilon_{AB})$.

The Hamiltonian (2) has nonlinear terms up to fourth order. It is usually hard to study the properties of this kind of system analytically, but in this model the Hamiltonian can be simplified in a restricted region of parameter space by making the following nonlinear transformation:

$$g_i=(n_i-\tau_i)^2\ . \tag{4}$$

It is clear that $g_i$ is unity if exactly one of the $A$ or $B$ components are present at the site $i$ and zero if they are both absent or both present. Hence, $g_i$ is an indicator of single occupancy at the site $i$. The sets of variables $\{g_i\}$ and $\{\tau_i\}$, or $\{g_i\}$ and $\{n_i\}$ are independent, since the transformation (4) can be inverted:

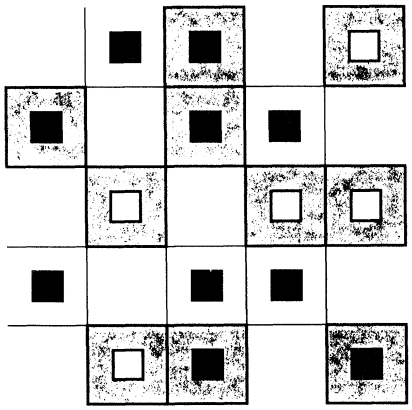

FIG. 1. A lattice model for an interacting binary reactant mixture. There are three kinds of particles, namely $A$ (square loops), $B$ (small dark squares), and a third composite particle $C$, which is formed when a $B$ and an $A$ particle are at the same site. Each particle interacts with other neighboring particles (see text).

$$n_i=(g_i-\tau_i)^2=g_i-\tau_i+2\gamma_i$$
$$\text{or } \tau_i=(g_i-n_i)^2=g_i-n_i+2\gamma_i\ . \tag{5}$$

We can thus eliminate either the $n_i$ or the $\tau_i$ variables in Eq. (2). Due to the symmetry between the $A$ and $B$ components in the Hamiltonian, we choose to eliminate the $n_i$ variables in the subsequent analysis without loss of generality. The model then becomes more tractable if we make the following constraints:

$$\mathcal{C}_1\left[\sum_{\langle ij\rangle}\gamma_i\gamma_j\right]=-\beta[4(\varepsilon_{AA}+\varepsilon_{AC})+\varepsilon_{CC}]=0\ ,$$
$$\mathcal{C}_2\left[\sum_{\langle ij\rangle}(g_i\gamma_j+\gamma_ig_j)\right]=-\beta[2\varepsilon_{AA}+\varepsilon_{AC}]=0\ ,$$
$$\mathcal{C}_3\left[\sum_{\langle ij\rangle}(\tau_i\gamma_j+\gamma_i\tau_j)\right]=-\beta[2(\varepsilon_{AB}-\varepsilon_{AA})+\varepsilon_{BC}-\varepsilon_{AC}]=0\ , \tag{6}$$
$$\mathcal{C}_4\left[\sum_{\langle ij\rangle}(g_i\tau_j+\tau_ig_j)\right]=-\beta[\varepsilon_{AB}-\varepsilon_{AA}]=0\ ,$$

where the $\mathcal{C}$'s denote coefficients. We will assume that these constraints always hold for the rest of this paper, implying that

$$\varepsilon_{CC}=-2\varepsilon_{AC}=-2\varepsilon_{BC}=4\varepsilon_{AB}=4\varepsilon_{AA}\ . \tag{7}$$

While it is true that this is a restriction on the original model (2), there still exists a rich variety of phases with the remaining freedom available. Using the constraints in Eq. (7), the partition function becomes

$$Z=\sum_{\{g_i\},\{\tau_i\}}\exp\left[-\beta\sum_{\langle ij\rangle}[\varepsilon_{AA}g_ig_j+(\varepsilon_{BB}-\varepsilon_{AA})\tau_i\tau_j]\right.$$
$$-\beta(2\mu_A+\mu_C)\sum_i g_i\tau_i$$
$$\left.+\beta\sum_i[\mu_Ag_i+(\mu_A+\mu_B+\mu_C)\tau_i]\right]\ . \tag{8}$$

This is the partition function of an interacting lattice gas of two species, whose Hamiltonian has no terms higher than of second order.

Let the densities of the components $A$, $B$, and $C$ be $\rho_A$, $\rho_B$, and $\rho_C$, respectively. They are given by

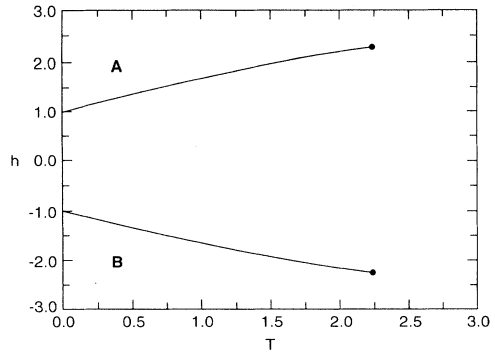


FIG. 2. A typical phase diagram for $\varepsilon_{AA}=\varepsilon_{BB}<0$ and $2\mu_0+\mu_C=0$. There are two first order lines ending at critical points. Here we have chosen $\varepsilon_{AA}+\mu_C/4=0.5$. The phase for small values of $|h|$ has $\rho_C\approx\frac{1}{2}$.

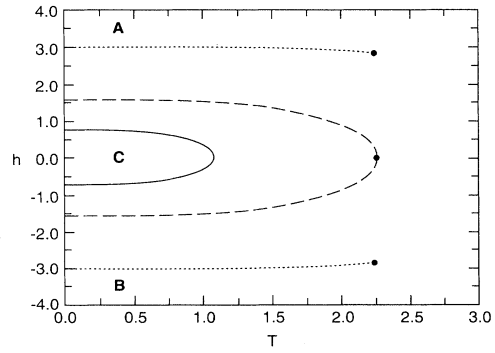


FIG. 3. Three kinds of phase diagrams for $\varepsilon_{AA}<0$ and $2\mu_0+\mu_C\neq 0$. Here we have chosen $\varepsilon_{AA}=\varepsilon_{BB}=-4$, $\mu_0=10$, and three values for $\mu_C$. (i) $\mu_C=-1.25$ (continuous line); (ii) $\mu_C=-0.427\,528$ (dashed line). The dark circle is a critical point; (iii) $\mu_C=1$ (dotted lines, both ending at critical points). There are similar graphs for $2\mu_0+\mu_C<0$, in which case the phase in the central region would be $D$.

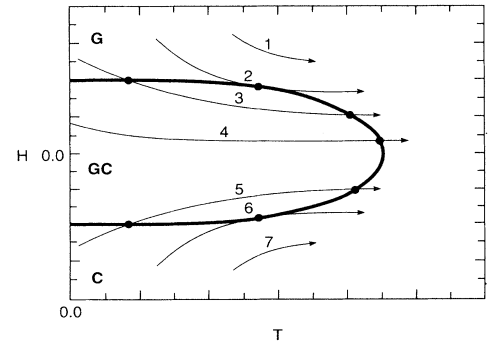


FIG. 4. Schematic plot of the seven possible cases for $\varepsilon_{AA}=\varepsilon_{BB}>0$. The dark curve is a critical line, and the seven light curves represent the possible paths the temperature dependent field $H$ can take, depending on the other parameters. For $h>0$, $G$ represents $A$ particles, while for $h<0$, $G$ represents $B$ particles.

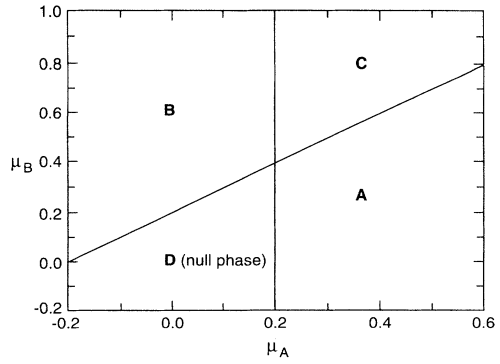


FIG. 5. A typical phase diagram for $\mu_C=-2\mu_A$, $\varepsilon_{AA}<0$ and $\varepsilon_{BB}<\varepsilon_{AA}$, at zero temperature. Both the lines correspond to first order phase transitions. In this figure $\varepsilon_{AA}=-0.1$, $\varepsilon_{BB}=-0.2$.

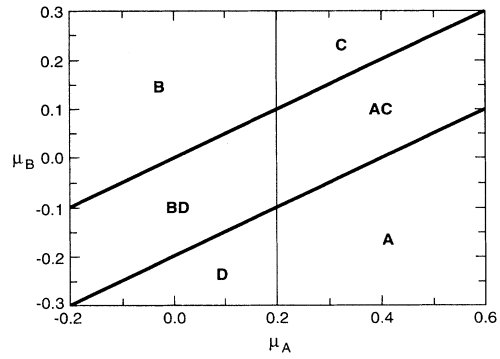


FIG. 6. A typical phase diagram for $\mu_C=-2\mu_A$, $\varepsilon_{AA}<0$, and $\varepsilon_{BB}>\varepsilon_{AA}$ at zero temperature. The two oblique lines correspond to second order phase transitions, while the vertical line is of first order. Here we have chosen $\varepsilon_{AA}=-0.1$, $\varepsilon_{BB}=0$.

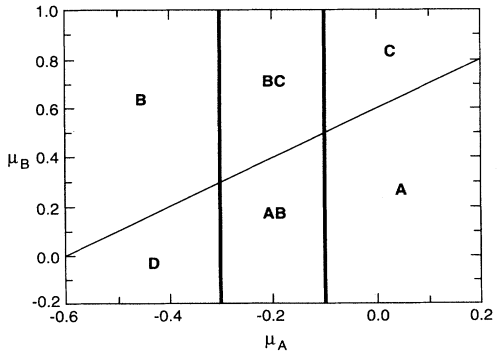


FIG. 7. A typical phase diagram for $\mu_C=-2\mu_A$, $\varepsilon_{AA}>0$, and $\varepsilon_{BB}<\varepsilon_{AA}$, at zero temperature. The two vertical line correspond to second order lines, while the oblique line is of first order. Our choice of parameters in this figure is $\varepsilon_{AA}=0.1$, $\varepsilon_{BB}=0$.

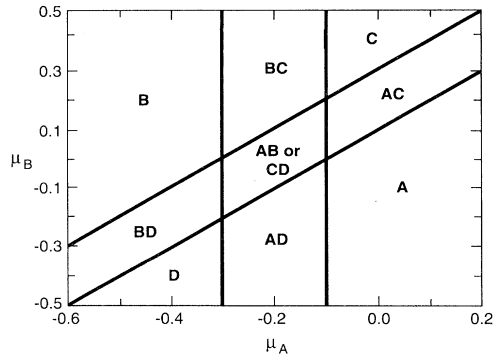


FIG. 8. A typical phase diagram for $\mu_C=-2\mu_A$, $\varepsilon_{AA}>0$, and $\varepsilon_{BB}>\varepsilon_{AA}$, at zero temperature. All the four lines correspond to second order phase transitions. The central parallelogram region can have a coexistence of two phases (see text). In this figure, $\varepsilon_{AA}=0.1$ and $\varepsilon_{BB}=0.2$.

$$\rho_A=\langle n_i(1-\tau_i)\rangle=\frac{1}{N\beta}\left[\frac{\partial \ln Z}{\partial \mu_A}-\frac{\partial \ln Z}{\partial \mu_C}\right],$$
$$\rho_B=\langle \tau_i(1-n_i)\rangle=\frac{1}{N\beta}\left[\frac{\partial \ln Z}{\partial \mu_B}-\frac{\partial \ln Z}{\partial \mu_C}\right], \tag{9}$$
$$\rho_C=\langle n_i\tau_i\rangle=\frac{1}{N\beta}\left[\frac{\partial \ln Z}{\partial \mu_C}\right].$$

In the next two sections, we study the two nontrivial cases $\varepsilon_{AA}=\varepsilon_{BB}$ and $\mu_C=-2\mu_A$. It is also possible to obtain the phase diagram when $\varepsilon_{AA}=0$. However, in the latter case it is clear from Eq. (7) that all the cubic and quartic nonlinear terms in the original Hamiltonian vanish, making the transformation (4) unnecessary.

Our main results for $\varepsilon_{AA}=\varepsilon_{BB}$ are summarized by the phase diagrams in Figs. 2, 3, and 4. If $\varepsilon_{AA}$ is attractive, then there are typically two first order transitions at low temperatures as the relative concentration of the components is varied. In some cases, the first order lines end in critical points (Figs. 2 and 3), while in other cases the first order lines enclose a third phase rich in C (Fig. 3), which is reminiscent of the Superconducting Cooper pair phase in BCS superconductors. If $\varepsilon_{AA}$ is repulsive, there is a critical boundary enclosing a sublattice phase (Fig. 4). Depending on the interaction parameters, there are zero, one, or two second order phase transitions in the system. Our main results for ($\mu_C=-2\mu_A$) are summarized in Figs. 5 to 8. There are sublattice phases when either $\varepsilon_{AA}$ or $\varepsilon_{BB}$ is repulsive (Figs. 6 and 7), or both (Fig. 8).

One general observation from all the cases we study is that sublattice phases are always separated from homogeneous phases by second order phase transitions, while homogeneous phases are separated from other homogeneous phases by first order phase transitions. In our model, sublattice phases can arise when there is a repulsive $A$-$A$ or $B$-$B$ interaction.

## III. PHASE DIAGRAMS FOR $\varepsilon_{AA}=\varepsilon_{BB}$

In this case the coefficient of $\sum\tau_i\tau_j$ vanishes. The partition function (8) can be rewritten as

$$Z=Z_g Z_B\ , \tag{10}$$

where $Z_g$ is the partition function of the $g$ particles along, and $Z_B$ is the partition of the $\tau$ particles, given any particular configuration of the $g$'s, i.e.,

$$Z_g=\sum_{\{g_i\}}\exp\left[-\beta\varepsilon_{AA}\sum_{\langle ij\rangle}g_ig_j+\beta\mu_A\sum_i g_i\right], \tag{11}$$

and

$$Z_B=\sum_{l_1=0}^{N_1}\sum_{l_2=0}^{N_2}{}^{N_1}C_{l_1}\,{}^{N_2}C_{l_2}\exp[\beta(\mu_A+\mu_B+\mu_C)l_1+\beta(\mu_B-\mu_A)l_2]$$
$$=\{1+\exp[\beta(\mu_A+\mu_B+\mu_C)]\}^{N_1}\{1+\exp[\beta(\mu_B-\mu_A)]\}^{N_2}\ . \tag{12}$$

Here $N_1$ is the maximum possible number of $B$ particles in sites distinct from those occupied by the $g$ variables, and $N_2$ is the maximum number of $B$ particles that occupies the same sites as the $g$ variables, i.e.,

$$N_1=N-\sum_i g_i\ , \tag{13}$$
$$N_2=\sum_i g_i\ .$$

Substituting Eqs. (13) in (12), we find that the partition function is

$$Z=\{1+\exp[\beta(\mu_A+\mu_B+\mu_C)]\}^N\sum_{\{g_i\}}\exp\left[-\beta\varepsilon_{AA}\sum_{\langle ij\rangle}g_ig_j\right]\exp\left[\left[-\beta\mu_C/2-\ln\frac{\cosh[\beta(\mu_A+\mu_B+\mu_C)/2]}{\cosh[\beta(\mu_A-\mu_B)/2]}\right]\sum_i g_i\right]. \tag{14}$$

It is useful to parametrize $\mu_A$ and $\mu_B$ as

$$\mu_A = \mu_0 + h \ , \qquad (15)$$
$$\mu_B = \mu_0 - h \ .$$

This parametrization expresses the symmetry between the particles $A$ and $B$ as a symmetry between $h$ and $-h$.

We can make the usual change of variables $g_i = (1+s_i)/2$ to obtain the spin variables $s_i$ for an Ising model. Let the corresponding Ising system have an effective coupling $J$ and an Ising field $H$:

$$J = \frac{\varepsilon_{AA}}{4} \ , \qquad (16)$$
$$H(T,h) = -\varepsilon_{AA} - \frac{1}{4}\mu_C - \frac{T}{2}\ln\left[\frac{\cosh(2\mu_0+\mu_C)/2T}{\cosh(h/T)}\right] .$$

We note that the Ising field is temperature dependent. It is clear that first order transitions are driven by the change in the sign of $H$, if $J$ is negative and the temperature is below the Ising critical temperature $T_C$. Hence the first order transition boundaries are exact in all dimensions.

Using Eqs. (9) and (14), one finds that the densities of the three components are given by

$$\rho_A = \tfrac{1}{4}(1+m_g)(1+\tanh\beta h) \ ,$$
$$\rho_B = \tfrac{1}{4}(1+m_g)(1-\tanh\beta h) \ , \qquad (17)$$
$$\rho_C = \tfrac{1}{4}(1-m_g)[1+\tanh\beta(\mu_0+\mu_C/2)] \ ,$$

where $m_g$ is the magnetization of the Ising system. The ratio of the components $A$ and $B$ is always given by $\rho_A/\rho_B = e^{2\beta h}$.

For the phase structure, there are three cases to be considered.

*Case (i):* $\varepsilon_{AA} < 0$; $2\mu_0 + \mu_C = 0$. In this case, the Ising model is ferromagnetic, and the Ising field $H$ decreases monotonically with increasing temperature for $|h| \neq 0$ and is constant otherwise. The condition for phase transitions to occur is that

$$H(\infty,0) = -\varepsilon_{AA} - \frac{\mu_C}{4} < 0 \ . \qquad (18)$$

In the $h$-$T$ plane there are two first order lines starting at $h = \pm 2H(0,0)$ and ending at a critical point, which is shown in Fig. 2. For small values of $|h|$, the low temperature phase is approximately half filled with the $C$ particles, and for large values of $|h|$, the low temperature phase consists of free particles. In particular, for $h$ large and positive, the low temperature phase is phase $B$ in obvious notation, and for $h$ large and negative, the low temperature phase is phase $A$. The extreme limit is when $\varepsilon_{AA} + \mu_C/4 = 0$, where both the first order lines collapse at $|h| = 0$ and end at $T_C$ with a critical point.

*Case (ii):* $\varepsilon_{AA} < 0$; $2\mu_0 + \mu_C \neq 0$. This also corresponds to a ferromagnetic Ising model, but in this case, the Ising field *increases* with temperature when $|h| < |\mu_0 + \mu_C/2|$. Hence in order for phase transitions to occur in the system, we require that

$$H(\infty,0) = -\varepsilon_{AA} - \frac{\mu_C}{4} > 0$$

and

$$H(0,0) = -\varepsilon_{AA} - \frac{\mu_C}{4} - \frac{1}{2}|\mu_0 + \mu_C/2| < 0 \ . \qquad (19)$$

When Eq. (19) is satisfied, the temperature at which the Ising field vanishes is maximum for $h = 0$. For nonzero values of $h$ the cross-over temperature decreases until, at the value $h_0 = -2H(0,0)$, it becomes zero. For $|h| > h_0$ there is no transition. The system has a first order transition if the Ising field sweeps through zero at any temperature below the critical temperature $T_C$ of the Ising system. There are thus three possible kinds of phase diagrams. If $H = 0$ at a crossover temperature smaller than $T_C$, then there is a continuous first order line that separates the two phases in the $h$-$T$ plane. If the cross-over temperature is larger than $T_C$, then the system has two first order lines, each ending at a critical point. If the crossover takes place exactly at $T_C$, then there is one critical point at the point where the two first order lines meet. In Fig. 3 we plot the phase diagram of the system in the $h$-$T$ plane for these three scenarios. Similar phase diagrams have been obtained in Ref. [10] at the mean field level, and also in a special case in three dimensions.

From Eq. (17) it is clear that at low temperatures and large values of $|h|$, the system has predominantly unreacted particles (corresponding to phase $A$ or $B$, depending on the sign of $h$). There are two possible low temperature phases, depending on whether $2\mu_0 + \mu_C$ is greater or less than zero. If $2\mu_0 + \mu_C > 0$, then the low temperature phase consists predominantly of the $C$ particles (phase $C$). On the other hand if $2\mu_0 + \mu_C < 0$, then the low temperature phase is predominantly empty of all the three types of particles, which we call the "null phase" and denote by phase $D$.

*Case (iii):* $\varepsilon_{AA} > 0$. In the cases (i) and (ii) above, we had $\varepsilon_{AA} < 0$. We now consider the antiferromagnetic case with $\varepsilon_{AA} > 0$, in which we get phases that are driven by *second* order phase transitions.

The simplest way to study this situation is to plot the phase diagram of the Ising antiferromagnet in a magnetic field. While the problem of an Ising antiferromagnet in an external magnetic field has not yet been solved exactly, the qualitative shape of the critical line is known for several lattice structures [13], and it is known to a high degree of precision in square lattices [14]. We have plotted it schematically in Fig. 4. The low temperature and large positive $H$ phase consists predominantly of unreacted particles. We call this the $G$ phase. The phase at low temperatures and large negative $H$ is phase $C$, with the density of $C$ particles being $e^{2\beta h}$. The phase at low temperatures and small $H$ has a sublattice structure, with predominantly unreacted particles in one sublattice such that $\rho_A/\rho_B = e^{2\beta h}$, and the other sublattice has a few unreacted particles and the density of the compound $C$ is given by $\rho_C = e^{2\beta h}$. This we denote by the phase $GC$.

In this case, $H$ is temperature dependent and varies in the same way as in cases (i) and (ii), except for a constant shift. Thus $H$ increases with increasing temperature when $|h|<|\mu_0+\mu_C/2|$ and decreases otherwise. There are thus totally seven possibilities, which we have illustrated in Fig. 4. In two of them, the system undergoes two second order phase transitions as the temperature is varied. This kind of behavior has been studied for a similar model in a *decorated* lattice [10]. There are of course the two special cases when the critical points merge, and this is discussed in some detail by Corrales and Wheeler [10]. Then there are also the two possibilities in which $H$ remains in the large positive region or in the large negative region at all temperatures, in which case there is no phase transition. Finally if $|H(0,h)|$ lies inside the sublattice section, there is exactly one second order phase transition in the system.

## IV. PHASE DIAGRAMS FOR $\mu_C=-2\mu_A$

We have so far considered the case when the coefficient of $\sum\tau_i\tau_j$ in Eq. (8) vanishes. It is also possible to obtain results when this coefficient is nonzero, provided the coefficient of $\sum g_i\tau_i$ vanishes, which happens when $\mu_C=-2\mu_A$. The system then becomes equivalent to two noninteracting lattice gases and can be transformed on to two noninteracting Ising models with effective couplings $J_g$ and $J_\tau$, and in the presence of magnetic fields $H_g$ and $H_\tau$, in the usual way. We then have

$$\begin{aligned} J_g&=\frac{\varepsilon_{AA}}{4}\ ,\\ J_\tau&=\tfrac{1}{4}(\varepsilon_{BB}-\varepsilon_{AA})\ ,\\ H_g&=\varepsilon_{AA}+\tfrac{1}{2}\mu_A\ ,\\ H_\tau&=(\varepsilon_{BB}-\varepsilon_{AA})+\tfrac{1}{2}(\mu_B-\mu_A)\ . \end{aligned} \tag{20}$$

We note that the Ising fields are not temperature dependent, which makes the analysis simpler as compared to that in the preceding section. The densities of the three components are given by

$$\begin{aligned} \rho_A&=\langle n_i(1-\tau_i)\rangle=\langle g_i(1-\tau_i)\rangle=\tfrac{1}{4}(1+m_g)(1-m_\tau)\ ,\\ \rho_B&=\langle \tau_i(1-n_i)\rangle=\langle g_i\tau_i\rangle=\tfrac{1}{4}(1+m_g)(1+m_\tau)\ ,\\ \rho_C&=\langle n_i\tau_i\rangle=\langle \tau_i(1-g_i)\rangle=\tfrac{1}{4}(1-m_g)(1+m_\tau)\ , \end{aligned} \tag{21}$$

where $m_g$ and $m_\tau$ are the magnetizations of the two Ising systems. One can verify that Eq. (21) is consistent with Eq. (17) for $\varepsilon_{AA}=\varepsilon_{BB}$, since in that case $m_\tau=-\tanh\beta h=\tanh\beta(\mu_0+\mu_C/2)$.

There are four cases, depending on whether each of the Ising models are ferromagnetic or antiferromagnetic.

*Case (i):* $\varepsilon_{AA}<0$, $\varepsilon_{BB}<\varepsilon_{AA}$. In this case both the systems are ferromagnetic. There are two critical points and four phases $A$, $B$,$C$ and the null phase $D$, which exist at temperatures below the lower of the critical temperatures. Let phase $I$ be the phase that is rich in $A$ type components. Phase $A$ is stable when $H_g>0$, $H_\tau<0$. Phase $B$ occurs when $H_g>0$, $H_\tau>0$. The phase $C$ occurs when $H_g<0$, $H_\tau>0$. The null phase (phase $D$) has a very low concentration of all the three substances $A$, $B$, and $C$, and occurs when $H_g<0$, $H_\tau<0$. The phase diagram in the plane of $\mu_A$ and $\mu_B$ is given in Fig. 5. The four regions are separated by first order phase boundaries. As the temperature is raised to the critical temperature of one of the models, the corresponding phase boundary becomes a critical line and vanishes at higher temperatures. Hence in this intermediate region there would be only two phases. At even higher temperatures, both the models become paramagnetic, and the other boundary line also disappears.

*Case (ii):* $\varepsilon_{AA}<0$, $\varepsilon_{BB}>\varepsilon_{AA}$. Here the Ising model for the $\tau$ variables is antiferromagnetic, while the other is ferromagnetic. Figure 6 is self-explanatory for this case and is the phase diagram at $T=0$. We note that the oblique phase boundaries are second order lines, and that there are totally six possible phases, including the two sublattice phases $BD$ and $AC$.

*Case (iii):* $\varepsilon_{AA}>0$, $\varepsilon_{BB}<\varepsilon_{AA}$. In this case the Ising model for the $g$ variables is antiferromagnetic, while the other is ferromagnetic. The phase diagram at zero temperature is given in Fig. 7. In this figure the oblique line is a first order line, while the two vertical lines are of second order. The two sublattice phases are $BC$ and $AD$.

*Case (iv):* $\varepsilon_{AA}>0$, $\varepsilon_{BB}>\varepsilon_{AA}$. This is the case in which both the models are antiferromagnetic and has the richest phase diagram. There are totally ten phases at low temperatures, which are shown in Fig. 8. In addition to the four phases $A$, $B$, $C$, and $D$, there are four sublattice phases $AC$, $AD$, $BC$, and $BD$. At the center of the phase diagram is a coexistence of two more sublattice phases $AB$ and $CD$. All the phases are separated by second order phase transitions. As the temperature is raised, the central boundary initially increases in size, then decreases until two of the lines pinch at the critical temperature of one of the models, leaving three phases in the intermediate region. At even higher temperatures there is only one phase.

## V. SUMMARY AND DISCUSSION

In summary, we have studied phase separation in an interacting binary reactant mixture. We have obtained the phase diagrams in some regions of parameter space by means of a nonlinear transformation. This enabled the model that had nontrivial interactions to be mapped on to coupled Ising models. The rich phase structure was thus seen to arise out of the various Ising ferromagnetic and antiferromagnetic phases.

In this paper we have studied equilibrium properties of the system. Since the transformation (4) can be made in all dimensions, our results are qualitatively correct in all dimensions greater than or equal to 2, and the first order transition boundaries are exact. The next step would be to study the dynamics of this system. Is it possible to make an analogous nonlinear transformation as was done here, which decouples variables for the dynamics also?

As is well known, one has more flexibility in defining dynamics that lead to the same equilibrium Boltzmann distribution. For example, one or more of the particles $A$, $B$, or $C$ can be kept immobile, while the others diffuse. The immobile practices can then be considered to be like "traps". Such dynamics in this model may shed some light on, for example, chemical reactions in a background of quenched random disorder. Another interesting possibility is the existence of glassy behavior in the system, perhaps in nonbipartite lattices. These are issues that we hope to address soon.

## ACKNOWLEDGMENTS

I would like to thank M. Barma and P. Bak for helpful discussions, and M. Paczuski for a critical reading of the manuscript. This work was supported by the Division of Material Sciences, U.S. Department of Energy, under Contract No. DE-AC02-76CH00016.

[1] D. Lombardo, F. Mallamace, N. Micali, and D'Arrigo, Phys. Rev. E **49**, 1430 (1994).
[2] E. Freysz, E. Laffon, J. P. Delville, and A. Ducasse, Phys. Rev. E **49**, 2141 (1994).
[3] *Statics and Dynamics of Alloy Phase Transitions,* edited by P. E. A. Turchi and A. Gonis (Plenum, New York, 1994).
[4] R. M. Neuman, Phys. Lett. **77A**, 55 (1980).
[5] *Phase Transitions in Surface Films 2,* edited H. Taub, G. Torzo, H. J. Lauter, and S. C. Fain, Jr. (Plenum, New York , 1991).
[6] For recent reviews of theoretical methods see A. Zunger, in *Statics and Dynamics of Alloy Phase Transitions* (Ref. [3]), pp. 361–419; K. Binder, *ibid.*, pp. 467–493; A Finel, *ibid.*, pp. 495–540.
[7] Some interesting model systems have been studied analytically; D. Frenkel and A. A. Louis, Phys. Rev. Lett. **68**, 3363 (1992); J. C. Lin and P. L. Taylor, Phys. Rev. E **49**, 2058 (1994).
[8] This has become textbook material; e.g., S. K. Ma, *Statistical Mechanics* (World Scientific, Singapore, 1985), p. 307.
[9] G. Inden, in *Statics and Dynamics of Alloy Phase Transitions* (Ref. [3]), pp. 17–43.
[10] L. R. Corrales and J. C. Wheeler, J. Chem Phys. **91**, 7097 (1989).
[11] Y. Albeck and M. Gitterman, Philos. Mag. **56**, 881 (1987).
[12] F. Schmid and K. Binder, J. Phys. Condens. Matter **4**, 3569 (1992).
[13] *Phase Transitions and Critical Phenomena, Vol. 3,* edited by C. Domb and M. S. Green (Academic, London, 1974), pp. 372–374.
[14] H. W. J. Blöte and Xue-Ning Wu, J. Phys. A **23**, L627 (1990).